NDT and E International 99 (2018) 64–71

Contents lists available at ScienceDirect

NDT and E International

journal homepage: www.elsevier.com/locate/ndteint

The sizing of small surface-breaking fatigue cracks using ultrasonic arrays

Chaoyong Peng[a,b,*], Long Bai[b], Jie Zhang[b], Bruce W. Drinkwater[b]

[a] School of Physical Science and Technology, Southwest Jiaotong University, Chengdu, 610031, China
[b] Department of Mechanical Engineering, University of Bristol, University Walk, Bristol, BS8 1TR, UK

ARTICLE INFO

Keywords:
Ultrasonic arrays
Defect sizing
Defect characterisation
Fatigue crack
Total focusing method
Scattering coefficient matrix

ABSTRACT

Using ultrasonic arrays to detect and characterise surface breaking cracks is important in the non-destructive evaluation (NDE) field. It can provide early warning of failure and useful information for component integrity assessment. Typically, cracks are approximated by machined slots and used to examine and assess defect detection and characterisation methods. In this paper, real surface breaking cracks are fabricated in 3-point bending specimens following ASTM standard E1820 and used to examine the performance of two array defect characterisation methods: image-based and scattering matrix sizing. In both cases, an array is used to record the full matrix capture (FMC). In image-based sizing, the total focusing method (TFM) is used to form an image from which the defect size is measured directly. This approach is shown to work well for cracks greater than two wavelengths in size. The FMC is also used to extract the defect scattering matrix which is then compared to a precomputed smooth-crack scattering matrix database. The best match between experiment and this database is found by cross-correlation and used to characterise the defect. This approach is shown to work well for defects in the range of 0.78–1.84 wavelengths. Within these ranges of applicability, both methods show excellent agreement between the known crack length and that measured ultrasonically, with errors less than 19% in all cases.

1. Introduction

Surface breaking cracks (SBCs) resulting from cyclic loading and harsh operating conditions are common in solid structures such as rail tracks, gears, pressure vessels and pipelines [1–6]. Using structural integrity assessment, combined with fracture mechanics calculations, the measured size of SBCs can be used to estimate the remaining life of the structure [7]. In non-destructive evaluation (NDE), there various techniques used to detect the indication of SBCs, for example, dye penetrant inspection, magnetic particle inspection, eddy current testing and thermography [8]. These techniques allow sizing if SBCs are on the accessible front surface of the test structure.

For detecting and sizing SBCs on the inaccessible back surface of components, ultrasonic guided wave or bulk wave inspection can be used. The guided waves technique is typically used to detect and size relatively large defects over a long distance [9–12]. Higher resolution, local inspection can be achieved using ultrasonic bulk wave inspection. Using these approaches, defect detection and characterisation measurements are often made by placing an oblique incidence bulk wave transducer or array on the front-wall of a structure to detect defects on the back-wall [13–29]. Array images can be formed either by traditional imaging approaches [13,14] or via recording the Full Matrix Capture (FMC) and application of post-processing techniques, e.g., the Total Focusing Method (TFM) [15] and its variants [16–18]. An important benefit of using ultrasonic arrays to detect and characterise SBCs is that one array transducer allows a given crack to be illuminated from a wide range of angles. The high resolution images formed increase the chances of detection [15,21] and the data can be further processed to extract the scattering behaviour which provides valuable characterisation information via the scattering coefficient matrix (S-matrix) [20,22]. For a defect with a size greater than approximately two wavelengths it has been shown that information contained within a TFM image can be used to measure crack size [13,18,23]. However, to date this approach has often been shown quantitatively using artificially machined notches [18], simulated rough defects [24] and large embedded real cracks [25,26], whose sizes are greater than 2.5 mm (2 wavelengths at 5 MHz). Alternatively, for cracks less than two wavelengths, it has been shown that the extracted S-matrix can be used for sizing [19,22,23] although this approach has only been experimentally explored on EDM notches whose sizes range from 1 mm to 3 mm (0.8–2.5 wavelength at 5 MHz).

In this paper we examine the performance of defect characterisation using array image-based and S-matrix based sizing techniques. In particular we explore their applicability to real SBCs grown in aluminium samples under 3-point bending. We consider inaccessible back-surface cracks for which bulk wave ultrasonic is the industry standard

---

[*] Corresponding author. School of Physical Science and Technology, Southwest Jiaotong University, Chengdu, 610031, China.
E-mail addresses: pengmd@163.com (C. Peng), lb13340@bristol.ac.uk (L. Bai), j.zhang@bristol.ac.uk (J. Zhang), b.drinkwater@bristol.ac.uk (B.W. Drinkwater).

https://doi.org/10.1016/j.ndteint.2018.06.005
Received 11 March 2018; Received in revised form 26 June 2018; Accepted 27 June 2018

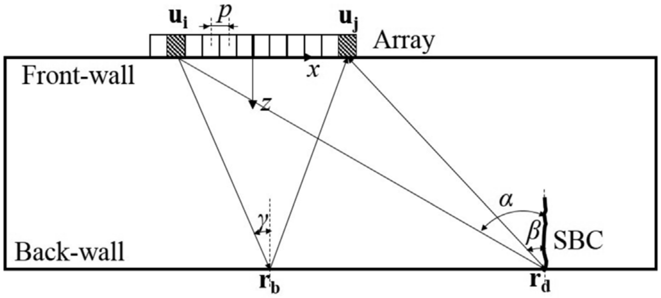

Fig. 1. Schematic diagram illustrating the geometry used in the hybrid forward scattering model.

technique [13,14,25]. The motivation is therefore to understand the measurement limitations of these new techniques on real defects and to assess if they offer advantages over the best existing techniques. This investigation on realistic defects therefore provides a further step towards the industrial uptake of these emerging techniques.

2. Modelled structure and S-matrix

2.1. Overview of the hybrid scattering model

In order to understand the performance of ultrasonic imaging of SBCs and explore methodologies for sizing them, a 2D hybrid scattering model [16,30] was used to simulate array data sets from a simple plate-like structure with a SBC. Here, a hybrid model is used to simulate the ultrasonic waves transmitted from each array element, propagating in a plate-like structure, interacting with both a planar back-wall surface and a SBC, and then received by the array elements.

Consider a 2D solid structure with the geometry shown in Fig. 1. The structure has isotropic material properties defined by the density ρ, longitudinal wave speed c_l and transverse wave speed c_t. Cartesian coordinates, (x, z), represent lateral position and depth with respect to the center of the 1D linear array. The figure also schematically shows two possible wave paths from a transmitter element located at $\mathbf{u_i}$ back to a receiver element located at $\mathbf{u_j}$. One wave path corresponds the wave reflected from the back-wall and it is reflected at $\mathbf{r_b}$ with the same incident and reflected angle γ with respect to the normal of the planar back-wall. The other wave path represents the scattered wave from the SBC at $\mathbf{r_d}$ with the incident angle, α, and the scattered angle, β, with respect to the normal of the planar back-wall. γ is a function of $\mathbf{u_i}$, $\mathbf{u_j}$ and $\mathbf{r_b}$ while α and β are the functions of $\mathbf{u_i}$, $\mathbf{u_j}$ and $\mathbf{r_d}$. Note that in this simulation, only the ultrasonic waves from longitudinal incident, reflected and scattered wave modes were considered although the SBC scattering matrix calculation solved the 2D elastodynamic scattering problem [10,20].

2.2. The far field defect S-matrix

The interaction between ultrasonic waves and a defect is encoded by its far field S-matrix which is defined as the far field complex amplitude of the signals from the crack as a function of the incident and scattered angles (α, β) [22,30,31]. When a plane wave of displacement amplitude u_{in} and propagation angle, α, is incident on a 2D SBC of length, a, the scattered field decays in inverse proportion to the square root of the distance from the crack in the far field. If the amplitude of the scattered wave at a distance r_{sc} along the scattered angle, β, is u_{sc}, then the far field S-matrix is given by Refs. [22,30],

$$S(a, f, \alpha, \beta) = \frac{u_{sc}}{u_{in}}\sqrt{\frac{r_{sc}}{\lambda}}\,exp(-ik(r_{sc}-\lambda)), \tag{1}$$

where, λ is the wavelength and k is the wavenumber ($k = 2\pi/\lambda$). In this paper, a numerical method using local FE modelling without absorbing regions [31] was used to simulate the scattering coefficient matrices (S-matrices) from various vertical smooth SBCs.

2.3. Hybrid forward model to simulate the scattered signals from a structure

The array data is predicted using the above discussed numerically calculated scattering matrix in combination with a classic frequency domain, linear systems model of the wave propagation [16,30]. For a SBC with a length a and located at $\mathbf{r_d}$ as shown in Fig. 1, in the frequency domain, the matrix of raw array data from this defect, $G_{ij}(f)$, received by the array element located at $\mathbf{u_j}$ when the element transmits at $\mathbf{u_i}$ can be written in the following general form [16,30],

$$G^d_{ij}(a,\ f,\ \mathbf{u_i},\ \mathbf{u_j},\ \mathbf{r_d}) = \frac{A(f)D(f,\ \alpha(\mathbf{u_i},\ \mathbf{r_d}))D(f,\ \beta(\mathbf{u_j},\ \mathbf{r_d}))S(a, f, \alpha(\mathbf{u_i},\ \mathbf{r_d}), \beta(\mathbf{u_j},\ \mathbf{r_d}))exp(ik(|\mathbf{u_i} - \mathbf{r_d}| + |\mathbf{u_j} - \mathbf{r_d}|))}{\sqrt{|\mathbf{u_i} - \mathbf{r_d}||\mathbf{u_j} - \mathbf{r_d}|}}, \tag{2}$$

where, the function $A(f)$ represents the combination of the frequency spectrum of the signal transmitted from the array controller instrument, D is the directivity of an array element [32].

Also shown in Fig. 1 is the wave path for a specular reflection from the planar back-wall of the sample occurring at position $\mathbf{r_b}$. In the frequency domain, the corresponding expression for the first back-wall echo is [16,30],

$$G^b_{ij}(f,\ \mathbf{u_i},\ \mathbf{u_j},\ \mathbf{r_b}) = \frac{A(f)D^2(f,\ \gamma(\mathbf{u_i},\ \mathbf{u_j},\ \mathbf{r_b}))R(\gamma(\mathbf{u_i},\ \mathbf{u_j},\ \mathbf{r_b}))exp(ik(|\mathbf{u_i} - \mathbf{r_b}| + |\mathbf{u_j} - \mathbf{r_b}|))}{\sqrt{|\mathbf{u_i} - \mathbf{r_b}| + |\mathbf{u_j} - \mathbf{r_b}|}}, \tag{3}$$

where, R is the longitudinal-longitudinal reflection coefficient [33]. Hence, the total array data from a SBC and the first back-wall reflection, $G(f,\ \mathbf{u_i},\ \mathbf{u_j})$, is,

$$G_{ij}(a, f, \mathbf{u_i}, \mathbf{u_j}) = G^d_{ij}(a, f, \mathbf{u_i}, \mathbf{u_j}, \mathbf{r_d}) + G^b_{ij}(f, \mathbf{u_i}, \mathbf{u_j}, \mathbf{r_b}). \tag{4}$$

The time domain data, $g_{ij}(t) = g_d(t) + g_b(t)$, can then be obtained using an inverse Fast Fourier Transform (IFFT) to build up a full simulated FMC data set for a SBC.

3. Sizing methodology for SBCs

Here, the image-based and S-matrix sizing methods are first explored on simulated array data using the hybrid model described briefly in section 2. The TFM [15] was chosen as an example of an ultrasonic array imaging algorithm for image-based sizing of SBCs. For a large SBC, the crack tip and crack mouth can be resolved in the ultrasonic image and hence the crack length can be measured [18]. However, for a small crack these image features merge and a single high intensity region close in shape to the point spread function (PSF) of the array imaging system is observed which is not suitable for sizing.

In the S-matrix sizing technique [22] the S-matrix of the crack is first extracted from the FMC array data set and then used to compare with a pre-computed smooth-crack S-matrix database. The best match between experiment and this database is found by cross-correlation and used to characterise the defect.

In the simulations, an ultrasonic array (i.e. #1 in Table 1) was placed on the front-wall of an aluminium plate of thickness 40 mm, longitudinal velocity $c_l = 6400$ m/s, transverse velocity $c_t = 3100$ m/s and density $\rho = 2700$ kg/m^3.

3.1. Image-based sizing technique

Fig. 2(a) and (b) compare the simulated TFM images for